STABLE CADENCE TRACKING OF ADMITTING FUNCTIONAL ELECTRICAL STIMULATION CYCLE

Christian A. Cousin *
Victor H. Duenas
Department of Mechanical
and Aerospace Engineering
University of Florida
Gainesville, Florida 32611
Email:{ccousin,vhduenas}@ufl.edu

Courtney A. Rouse
Warren E. Dixon
Department of Mechanical
and Aerospace Engineering
University of Florida
Gainesville, Florida 32611
Email:{courtneyarouse,wdixon}@ufl.edu

ABSTRACT

Rehabilitation robotics and functional electrical stimulation (FES) are two promising methods of rehabilitation for people with neurological disorders. In motorized FES cycling, both the rider and the motorized cycle must be controlled for cooperative human-machine interaction. While rehabilitation goals vary widely, FES cycling traditionally rejects rider disturbances to accomplish cadence and power tracking; however, this paper ensures that the cycle accommodates the rider without rejecting rider disturbances as a means to promote function and strength recovery while ensuring rider safety. A cadence and admittance controller are developed to activate the cycle's electric motor and the rider's leg muscles through FES when kinematically efficient. Using a single set of combined cycle-rider dynamics, a Lyapunov-like switched systems analysis is conducted to conclude global exponential cadence tracking. A subsequent passivity analysis is conducted to show the admittance controller is passive with respect to the rider. For a desired cadence of 50 RPM, preliminary experiments on one able-bodied participant and one participant with spina bifida demonstrate tracking errors of -0.07±2.59 RPM and -0.20±3.86 RPM, respectively.

*Address all correspondence to this author.

INTRODUCTION[1]

Lower-limb functional electrical stimulation (FES) cycling is a promising rehabilitation strategy for people with neurological disorders (e.g., spinal cord injury, stroke, traumatic brain injury, Parkinson's, etc.). FES cycling can be accomplished with or without an electric motor (cf. [1] and [2], respectively). In motorized FES cycling, a rider's muscles are artificially contracted using neuromuscular electrical stimulation to pedal the cycle in coordination with an electric motor, combining the benefits of FES (increased muscle mass, bone mineral density, etc. [3, 4]) and rehabilitation robots (increased somatosensory stimulation, motor function, etc. [5]). By adding the motor to the cycle, additional control authority is granted to the system and unique objectives can be investigated, such as cadence and power tracking [6], instead of cadence tracking alone [2]. However, motorized FES cycling has numerous challenges such as lower metabolic efficiency compared to volitional cycling, nonphysiological muscle recruitment, and poor coordination of the muscle groups [7–9]. Furthermore, motorized FES cycling requires a controller to be designed for both the muscles and motor, and depending on the cycling objective (i.e., cadence or cadence and power tracking), human-machine interactions must be considered since actuators may be applying torques against each other.

Despite these challenges, FES cycling is often achieved through open-loop methods in practice (cf. [10, 11]); however,

[1]This research is supported in part by the National Science Foundation Graduate Research Fellowship Program under Grant No. DGE-1315138 and AFOSR award number FA9550-18-1-0109. Any opinions, findings and conclusions, or recommendations expressed in this material are those of the author(s) and do not necessarily reflect the views of the sponsoring agency.

numerous studies exist where closed-loop control is applied with adaptive [2, 12] or robust methods [1, 13] for guaranteed performance and improved responsiveness. Additional investigation is warranted for the human-machine interaction that arises during closed-loop motorized FES, particularly when the motor and muscles are stimultaneously activated, because undesirable interactions may result. Therefore, the objectives must be prioritized. Admittance control, pioneered by Hogan in [14], offers an intuitive solution to this problem; instead of explicitly regulating position or force, it regulates dynamic behavior. Admittance control has been used in numerous applications involving human-machine interaction, particularly with rehabilitation [15], where the robots modify their behavior based on the interaction forces with the human. Human-machine interaction must be thoroughly examined because individuals with neurological conditions often have weakened, unreliable, and/or unpredictable movements [16].

In traditional nonlinear position/cadence control, stability in the sense of Lyapunov is often employed to show regulation of the tracking errors [17]. When two controllers are applying torques in opposite directions, an analysis tool known as passivity is employed to prove stability; passive systems are systems which are dissipative in nature and do not self-excite (i.e., they do not generate more energy than injected) [17]. Previous FES cycling approaches without admittance have utilized Lyapunov-like switched systems analyses to ensure stabililty of both the human and machine [1, 2, 6, 12, 13, 18–20], since their tracking objectives compliment each other (e.g., cadence and power) as opposed to conflict (e.g., different desired cadences). Other studies have been conducted on the upper body to show stable interactions can be obtained with differing trajectories when combined with passive controllers [21].

In this paper, an admittance and cadence controller are developed for an FES cycle. Because the admittance controller uses an inner-loop position-based controller, if the admitted trajectory differs from the desired trajectory, unstable behavior may result as the two controllers will attempt to minimize two different error systems. Hence, the admittance control is designed to be passive with respect to the cadence controller such that it yields to the interaction torques. When the cadence controller is used to stimulate the rider's muscles, the admittance controller is employed on the cycle's motor to ensure safe human-machine interaction while still providing guidance toward the control objective. A single set of nonlinear, uncertain combined cycle-rider dynamics are utilized in conjunction with a Lyapunov-like switched systems stability analysis to conclude global exponential tracking of the cadence objective and a passivity analysis is conducted to conclude passivity of the admittance controller with respect to the rider. Preliminary experiments on one able-bodied participant and one participant with spina bifida demonstrate tracking errors of -0.07±2.59 RPM and -0.20±3.86 RPM, respectively.

DYNAMICS

The combined cycle-rider dynamics can be modeled as [13]

$$\begin{aligned}\tau_m(q,\dot{q},t)+\tau_e(q,\dot{q},t) &= \\ &M(q)\ddot{q}+V(q,\dot{q})\dot{q}+G(q)+P(q,\dot{q})+b\dot{q}+d(t),\end{aligned} \quad (1)$$

where $q:\mathbb{R}_{\geq 0}\to\mathcal{Q}$, $\dot{q}:\mathbb{R}_{\geq 0}\to\mathbb{R}$, and $\ddot{q}:\mathbb{R}_{\geq 0}\to\mathbb{R}$ denote the measurable crank angle, calculable velocity, and acceleration, respectively, and $\mathcal{Q}\subseteq\mathbb{R}$ denotes the set of possible crank angles. The torque inputs consist of the contribution from the rider's leg muscles, denoted by $\tau_m:\mathcal{Q}\times\mathbb{R}\times\mathbb{R}_{\geq 0}\to\mathbb{R}$, and the cycle's electric motor, denoted by $\tau_r:\mathcal{Q}\times\mathbb{R}\times\mathbb{R}_{\geq 0}\to\mathbb{R}$. The combined inertial, centripetal-Coriolis, and gravitational effects of the rider's legs and cycle are denoted by $M:\mathcal{Q}\to\mathbb{R}$, $V:\mathcal{Q}\times\mathbb{R}\to\mathbb{R}$, and $G:\mathcal{Q}\to\mathbb{R}$, respectively. The torque contribution from the rider's passive viscoelastic tissue forces and cycle's friction are denoted by $P:\mathcal{Q}\times\mathbb{R}\to\mathbb{R}$ and $b:\mathbb{R}_{>0}\to\mathbb{R}$, respectively. System disturbances are denoted by $d:\mathbb{R}_{\geq 0}\to\mathbb{R}$. The rider's muscle torque contribution can be written as the sum of the large muscle groups of the legs (quadriceps, hamstrings, gluteals), given by [2]

$$\tau_m \triangleq B_M u_M, \quad (2)$$

$$B_M \triangleq \sum_{m\in\mathcal{M}} b_m k_m \sigma_m, \quad (3)$$

$\forall m\in\mathcal{M}$, where b_m, $B_M:\mathcal{Q}\times\mathbb{R}\to\mathbb{R}_{>0}$ denote the individual and lumped muscle control effectiveness, respectively, $\sigma_m:\mathcal{Q}\to\{0,1\}$ denotes the individual switching signal for each muscle group, $k_m\in\mathbb{R}_{>0}$ denotes the constant control gain for each muscle group, $u_M:\mathcal{Q}\times\mathbb{R}\times\mathbb{R}_{\geq 0}\to\mathbb{R}$ is the subsequently designed muscle stimulation current, and the subscript $m\in\mathcal{M}=\{RQ,RG,RH,LQ,LG,LH\}$ indicates the right (R) and left (L) quadriceps femoris (Q), gluteal (G), and hamstring (H) muscle groups, respectively. As in results such as [1, 13, 18, 19, 22], FES cycling is accomplished through alternating activation of the rider's muscles and/or the cycle's electric motor with continuously evolving state dynamics. Hence, FES cycling is an example of a state-dependent switched system. However, the rider's muscles can not be arbitrarily activated or back-pedaling, stalling, or early onset fatigue may occur. As such, the rider's muscles are coordinated (i.e., activated) using the piecewise right-continuous switching signal defined as

$$\sigma_m \triangleq \begin{cases} 1 & q\in\mathcal{Q}_m \\ 0 & q\notin\mathcal{Q}_m \end{cases}, \quad (4)$$

$\forall m\in\mathcal{M}$, where $\mathcal{Q}_m\subset\mathcal{Q}$ denotes the kinematically efficient region for each muscle group to transfer positive torque to the

[2]For notational brevity, all functional dependencies are hereafter suppressed unless required for clarity of exposition.

crank, designed as in [13]. The union of all muscle regions establishes the FES region of the crank cycle, defined as $\mathcal{Q}_M \triangleq \bigcup_{m\in\mathcal{M}} \mathcal{Q}_m$, with the kinematic deadzone (KDZ) region as the remainder. The electric motor's torque contribution in (1) can be modeled as

$$\tau_e \triangleq B_e\left(\sigma_M u_1 + (1-\sigma_M)\, u_2\right), \tag{5}$$

$$B_e \triangleq b_e k_e, \tag{6}$$

where the known motor control constant, $b_e \in \mathbb{R}_{>0}$, relates the motor's input current to output torque, $k_e \in \mathbb{R}_{>0}$ denotes a constant control gain, and $u_1,\ u_2 : \mathcal{Q}\times\mathbb{R}\times\mathbb{R}_{\geq 0} \to \mathbb{R}$, denote the subsequently designed admittance and cadence control inputs, respectively. Although the motor is active in both regions, when the crank is in the FES region, the cycle's motor behaves as an admittance whose control input is activated via the switching signal $\sigma_M : \mathcal{Q} \to \{0,\ 1\}$; else, the electric motor is utilized to track cadence and advance the crank until it returns to the FES region where the rider's muscles can be stimulated again. The motor's switching signal is dictated through the following relation

$$\sigma_M \triangleq \begin{cases} 1 & q \in \mathcal{Q}_M \\ 0 & q \notin \mathcal{Q}_M \end{cases}. \tag{7}$$

Substituting (2) and (5) into (1) yields the switched system dynamics

$$B_M u_M + B_e\left(\sigma_M u_1 + (1-\sigma_M)\, u_2\right) = M\ddot{q} + V\dot{q} + G + P + b\dot{q} + d. \tag{8}$$

The combined system in (8) has the following properties [18].

Property 1. $c_m \leq M \leq c_M$, where $c_m, c_M \in \mathbb{R}_{>0}$ are known constants.

Property 2. $|V| \leq c_V\,|\dot{q}|$, where $c_V \in \mathbb{R}_{>0}$ is a known constant.

Property 3. $|G| \leq c_G$, where $c_G \in \mathbb{R}_{>0}$ is a known constant.

Property 4. $|P| \leq c_{P1} + c_{P2}\,|\dot{q}|$, where $c_{P1}, c_{P2} \in \mathbb{R}_{>0}$ are known constants.

Property 5. $b \leq c_b$, where $c_b \in \mathbb{R}_{>0}$ is a known constant.

Property 6. $|d| \leq c_d$, where $c_d \in \mathbb{R}_{>0}$ is a known constant.

Property 7. $\dot{M} - 2V = 0$, by skew-symmetry.

Property 8. The unknown function relating stimulation current to torque is lower bounded by $B_{\underline{M}} \leq B_M$, where $B_{\underline{M}} \in \mathbb{R}_{>0}$ is a known constant.

CONTROL DEVELOPMENT

Cadence Controller

Cadence tracking will be accomplished by using the rider's muscles in the FES region and the cycle's electric motor in the KDZ regions. The cadence tracking objective is quantified by $e : \mathbb{R}_{\geq 0} \to \mathbb{R}$, and $r : \mathbb{R}_{\geq 0} \to \mathbb{R}$, each defined as

$$e \triangleq q_d - q, \tag{9}$$

$$r \triangleq \dot{e} + \alpha e, \tag{10}$$

where $q_d : \mathbb{R}_{\geq 0} \to \mathcal{Q}$ denotes the desired position, $\dot{q}_d : \mathbb{R}_{\geq 0} \to \mathbb{R}$ denotes the desired cadence, designed to be sufficiently smooth (i.e., $q_d(t),\ \dot{q}_d(t),\ \ddot{q}_d(t) \in \mathcal{L}_\infty$), and $\alpha \in \mathbb{R}_{>0}$ a constant control gain. The open-loop dynamics are obtained by taking the derivative of (10), premultiplying by M, adding and subtracting e, then substituting (8) and (10) to yield

$$M\dot{r} = \begin{cases} \chi_1 - B_M u_M - B_e u_1 - Vr - e & q \in \mathcal{Q}_M \\ \chi_1 - B_e u_2 - Vr - e & q \notin \mathcal{Q}_M \end{cases}, \tag{11}$$

where the switching relations in (4) and (7) were used to simplify control inputs based on the crank angle. The lumped auxiliary signal $\chi_1 : \mathcal{Q}\times\mathbb{R}\times\mathbb{R}_{\geq 0} \to \mathbb{R}$ is defined as $\chi_1 \triangleq M\left(\ddot{q}_d + \alpha r - \alpha^2 e\right) + V\left(\dot{q}_d + \alpha e\right) + G + P + b\left(\dot{q}_d - r + \alpha e\right) + d + e$. From Properties 1-6, χ_1 is bounded as

$$|\chi_1| \leq c_1 + c_2\,\|z\| + c_3\,\|z\|^2,$$

where $c_1,\ c_2,\ c_3 \in \mathbb{R}_{>0}$ are known constants, $\|\cdot\|$ denotes the standard Euclidean norm, and the error vector $z \in \mathbb{R}^2$ is defined as $z \triangleq [e,\ r]^T$. Based on (11), the region of the crank, and the subsequent stability analysis, the cadence controllers are designed as

$$u_M \triangleq \frac{1}{B_{\underline{M}}}\left[k_1 r + \left(k_2 + k_3\,\|z\| + k_4\,\|z\|^2 + k_5\,|u_1|\right)\operatorname{sgn}(r)\right], \tag{12}$$

$$u_2 \triangleq \frac{1}{B_e}\left[k_1 r + \left(k_2 + k_3\,\|z\| + k_4\,\|z\|^2\right)\operatorname{sgn}(r)\right], \tag{13}$$

where $k_i \in \mathbb{R}_{>0}\ \forall i = 1,\ 2,\ \ldots, 5$ denote constant control gains, $\operatorname{sgn}(\cdot)$ denotes the signum function, and $B_{\underline{M}}$ is developed in Property 8. Substituting (12) and (13) into (11) yields the closed-loop cadence error system

$$M\dot{r} = \begin{cases} \chi_1 - B_e u_1 - Vr - e - \frac{B_M}{B_{\underline{M}}}\Big[k_1 r \\ \quad + \Big(k_2 + k_3\,\|z\| + k_4\,\|z\|^2 \\ \quad + k_5\,|u_1|\Big)\operatorname{sgn}(r)\Big] & q \in \mathcal{Q}_M \\ \\ \chi_1 - Vr - e - \Big[k_1 r + \Big(k_2 + k_3\,\|z\| \\ \quad + k_4\,\|z\|^2\Big)\operatorname{sgn}(r)\Big] & q \notin \mathcal{Q}_M \end{cases}. \tag{14}$$

Admittance Controller

While in the FES regions, the rider's muscles are responsible for tracking cadence, and the motor for tracking a desired admittance. The cycle's admittance behavior is generated by the desired interaction dynamics, given by

$$\tau_{int} \triangleq M_d \ddot{q}_a + B_d \dot{q}_a, \tag{15}$$

where $\tau_{int} : \mathbb{R}_{\geq 0} \to \mathbb{R}$ is the measurable interaction torque between the rider and cycle, $q_a : \mathbb{R}_{\geq 0} \to \mathbb{R}$, $\dot{q}_a : \mathbb{R}_{\geq 0} \to \mathbb{R}$, and $\ddot{q}_a : \mathbb{R}_{\geq 0} \to \mathbb{R}$ denote the admitted position, velocity, and acceleration, respectively, and $M_d,\ B_d \in \mathbb{R}_{>0}$ denote the desired inertia and damping parameters, respectively, selected such that the transfer function of (15) is strictly positive real, i.e., passive [17, Lemma 6.4]. The following assumption is made with regard to the interaction torque.

Assumption 1. The measurable interaction torque is bounded (i.e., $\tau_{int} \in \mathcal{L}_\infty$) [23].

Remark 1. When combining the rider and cycle dynamics, the equal and opposite interaction torques, τ_{int}, cancel out. However, the interaction is still present and may be used in feedback.

Because the admittance manifests itself as a modified trajectory, an inner loop position controller is required. This controller tracks the admittance error system quantified by $\xi : \mathbb{R} \to \mathbb{R}$ and $\psi : \mathbb{R} \to \mathbb{R}$, defined as

$$\xi \triangleq q_a + q_d - q, \tag{16}$$

$$\psi \triangleq \dot{\xi} + \beta\xi. \tag{17}$$

The open-loop admittance error system is generated by taking the time derivative of (17), premultiplying by M, adding and subtracting ξ, and substituting (2), (7), (8), (16), and (17) to yield

$$M\dot{\psi} = \chi_2 - B_e u_1 - \tau_m - V\psi - \xi, \tag{18}$$

where the lumped auxiliary signal $\chi_2 : \mathcal{Q} \times \mathbb{R} \times \mathbb{R}_{\geq 0} \to \mathbb{R}$ is defined as $\chi_2 \triangleq M\left(\ddot{q}_a + \ddot{q}_d + \beta\psi - \beta^2\xi\right) + V\left(\dot{q}_d + \beta\xi + \dot{q}_a\right) + G + P + b\left(\dot{q}_d + \dot{q}_a - \psi + \beta\xi\right) + d + \xi$ and bounded by Properties 1-6 and Assumption 1 as

$$|\chi_2| \leq c_4 + c_5||\phi|| + c_6||\phi||^2,$$

where $c_4,\ c_5,\ c_6 \in \mathbb{R}_{>0}$ are known constants, and the error vectors $\phi \in \mathbb{R}^4$ and $\zeta \in \mathbb{R}^2$ are defined as $\phi \triangleq \left[\zeta^T,\ \dot{q}_a,\ \ddot{q}_a\right]^T$ and $\zeta \triangleq [\xi,\ \psi]^T$, respectively. Based on (18) and the subsequent stability analysis, the admittance controller is designed as

$$u_1 \triangleq \frac{1}{B_e}\left[k_6\psi + \left(k_7 + k_8\|\phi\| + k_9\|\phi\|^2\right)\operatorname{sgn}(\psi)\right], \tag{19}$$

where $k_i \in \mathbb{R}_{>0}\ \forall i = 6,\ 7,\ 8\ ,9$ denote constant control gains. Substituting (19) into (18) yields the closed-loop admittance error system

$$\begin{aligned} M\dot{\psi} = {} & \chi_2 - \tau_m - V\psi - \xi \\ & - \left[k_6\psi + \left(k_7 + k_8\|\phi\| + k_9\|\phi\|^2\right)\operatorname{sgn}(\psi)\right]. \end{aligned} \tag{20}$$

STABILITY ANALYSIS

To conclude stability of the cadence error system, the closed-loop error system must be evaluated within the FES and KDZ regions, then examined for destabilizing switching effects. Theorem 1 leverages a common Lyapunov function across both regions of the crank cycle, which by [24] guarantees overall system stability despite arbitrary switching. Theorem 2 leverages a storage function to prove the admittance error system is passive to the rider's muscle torque in the FES regions. For the following theorems, let $\underline{\lambda},\ \overline{\lambda},\ \Lambda$ and $\Gamma \in \mathbb{R}_{>0}$ denote known constants defined as $\underline{\lambda} \triangleq \min\left(\frac{c_m}{2},\ \frac{1}{2}\right)$, $\overline{\lambda} \triangleq \max\left(\frac{c_M}{2},\ \frac{1}{2}\right)$, $\Lambda \triangleq \frac{1}{\overline{\lambda}}\min\left(k_1,\ \alpha\right)$, and $\Gamma \triangleq \frac{1}{\overline{\lambda}}\min\left(k_6,\ \beta\right)$. Additionally, let $V_1,\ V_2 : \mathbb{R}^2 \to \mathbb{R}$ denote the continuously differentiable, positive definite Lyapunov function candidate and storage function, respectively, defined as

$$V_1 \triangleq \frac{1}{2}Mr^2 + \frac{1}{2}e^2, \tag{21}$$

$$V_2 \triangleq \frac{1}{2}M\psi^2 + \frac{1}{2}\xi^2, \tag{22}$$

which satisfy the following inequalities, respectively:

$$\underline{\lambda}\|z\|^2 \leq V_1 \leq \overline{\lambda}\|z\|^2. \tag{23}$$

$$\underline{\lambda}\|\zeta\|^2 \leq V_2 \leq \overline{\lambda}\|\zeta\|^2. \tag{24}$$

Theorem 1. *Given the closed-loop error systems in (14), global exponential tracking is guaranteed in the sense that*

$$\|z\| \overset{a.e.}{\leq} \sqrt{\frac{\overline{\lambda}}{\underline{\lambda}}}\|z(t_0)\|\exp\left[-\frac{\Lambda}{2}(t - t_0)\right], \tag{25}$$

$\forall t \in [t_0,\ \infty)$, *provided the following constant gain conditions are satisfied:*

$$k_2 \geq c_1,\ k_3 \geq c_2,\ k_4 \geq c_3,\ k_5 \geq B_e. \tag{26}$$

Proof. Let $z(t)$ for $t \in [t_0,\ \infty)$ be a Filippov solution to the differential inclusion $\dot{z} \in K[h_1](z)$, where $K[\cdot]$ is defined as in [25], and where $h_1 : \mathbb{R}^2 \to \mathbb{R}^2$ is defined using (10) and (14), as

$$h_1 \triangleq \begin{bmatrix} \dot{e} \\ \dot{r} \end{bmatrix}. \tag{27}$$

The time derivative of (21) exists almost everywhere (a.e.) (i.e., for almost all $t \in [t_0, \infty)$), and $\dot{V}_1(z) \overset{\text{a.e.}}{\in} \dot{\tilde{V}}_1(z)$, where $\dot{\tilde{V}}_1$ is the generalized time derivative of (21) along the Filippov trajectories of $\dot{z} = h_1(z)$ and is defined as in [26] as $\dot{\tilde{V}}_1 \triangleq \bigcap_{\xi \in \partial V_1(z)} \xi^T K \left[h_1(z)\ 1 \right]^T$, where ∂V_1 is the Clarke generalized gradient of V_1. Since V_1 is continuously differentiable in z, $\partial V_1 = \{\nabla V_1\}$ and $\dot{\tilde{V}}_1 \subseteq \left[e\ \ Mr\ \ \frac{1}{2} r \dot{M} r \right] K \left[h_1(z)\ 1 \right]^T$. Using the calculus of $K[\cdot]$ from [26], and substituting (10), (11), and (27) into the result, and using Property 7, yields

$$\dot{\tilde{V}}_1 \subseteq r\Big(\chi_1 - K[B_M u_M] - B_e\Big(K[\sigma_M u_1] + K\Big[\Big(1 - \sigma_M\Big) u_2\Big]\Big) - e\Big) + e(r - \alpha e). \tag{28}$$

Performing cancellations and using Property 7 allows (28) to be evaluated in the FES regions as

$$\dot{\tilde{V}}_1 \subseteq -\alpha e^2 + r\left(\chi_1 - K[B_M u_M] - B_e K[u_1]\right). \tag{29}$$

After using (12), (29) can be rewritten as

$$\dot{\tilde{V}}_1 \subseteq -\alpha e^2 + r\chi_1 - \frac{K[B_M]}{B_{\underline{M}}}\Big(k_1 r^2 + \Big(k_2 + k_3 \|z\| + k_4 \|z\|^2 + k_5 K[|u_1|]\Big)|r|\Big) - r B_e K[u_1], \tag{30}$$

where $K[\operatorname{sgn}(\cdot)] = \operatorname{SGN}(\cdot)$ such that $\operatorname{SGN}(\cdot) = \{1\}$ if $(\cdot) > 0$, $[-1, 1]$ if $(\cdot) = 0$, and $\{-1\}$ if $(\cdot) < 0$. Using Properties 1-6 and 8 and since $\dot{V}_1(z) \overset{\text{a.e.}}{\in} \dot{\tilde{V}}_1(z)$, (30) can be upper bounded as

$$\dot{V}_1 \overset{\text{a.e.}}{\leq} -\alpha e^2 - k_1 r^2 - |r|\Big(\lambda_1 + \lambda_2 \|z\| + \lambda_3 \|z\|^2 + \lambda_4 K[|u_1|]\Big), \tag{31}$$

where $\lambda_1, \lambda_2, \lambda_3, \lambda_4 \in \mathbb{R}$ are defined as $\lambda_1 \triangleq k_2 - c_1$, $\lambda_2 \triangleq k_3 - c_2$, $\lambda_3 \triangleq k_4 - c_3$, and $\lambda_4 \triangleq k_5 - B_e$. Provided the gain conditions in (26) are satisfied, $\lambda_1, \lambda_2, \lambda_3, \lambda_4 \geq 0$; thus, (31) can be upper bounded as

$$\dot{V}_1 \overset{\text{a.e.}}{\leq} -\Lambda V_1, \tag{32}$$

where Λ was defined previously. Similarly, for the KDZ region (i.e, $q \notin Q_M$), (28) is evaluated using (11) to yield

$$\dot{\tilde{V}}_1 \subseteq -\alpha e^2 + r\left(\chi_1 - B_e K[u_2]\right). \tag{33}$$

By using (13), (33) can be rewritten as

$$\dot{\tilde{V}}_1 \subseteq -\alpha e^2 + r\chi_1 - k_1 r^2 - \Big(k_2 + k_3 \|z\| + k_4 \|z\|^2\Big)|r|. \tag{34}$$

Using Properties 1-6 allows (34) to be upper bounded as

$$\dot{V}_1 \overset{\text{a.e.}}{\leq} -\alpha e^2 - k_1 r^2 - |r|\Big(\lambda_1 + \lambda_2 \|z\| + \lambda_3 \|z\|^2\Big), \tag{35}$$

where $\lambda_1, \lambda_2, \lambda_3$ maintain their previous definition. Provided the gain conditions in (26) are satisfied, (35) can be upper bounded as (32). Based on (23) and (32) the result in (25) can be obtained, and from the closed-loop error systems and Assumption 1, the cadence controllers in (12) and (13) are bounded. □

For the following theorem, let $t_n^M \in \mathbb{R}_{\geq 0}$ denote the time the crank enters Q_M of cycle n, and $t_n^K \in \mathbb{R}_{\geq 0}$ as the time the crank exits Q_M of cycle n.

Theorem 2. *Given the closed-loop error system in (20) and the admittance relation in (15), when $q \in Q_M$ the robot is passive from input $|\tau_m|$ to output $|\psi|$ and the robot error system is globally exponentially stable when in isolation (i.e., $\tau_m = 0$) in the sense that*

$$\|z\| \overset{a.e.}{\leq} \sqrt{\frac{\bar{\lambda}}{\underline{\lambda}}} \left\| z(t_n^M) \right\| \exp\left[-\frac{\Gamma}{2}(t - t_n^M) \right], \tag{36}$$

$\forall t \in \left[t_n^M, t_n^K\right)$ $\forall n$, where $\underline{\lambda}$, $\bar{\lambda}$ and Γ were defined previously, provided the following constant gain conditions are satisfied:

$$k_7 \geq c_4,\ k_8 \geq c_5,\ k_9 \geq c_6. \tag{37}$$

Proof. Let $\zeta(t)$ for $t \in \left[t_n^M, t_n^K\right)$ be a Filippov solution to the differential inclusion $\dot{\zeta} \in K[h_2](\zeta)$, where $K[\cdot]$ is defined as previously, and where $h_2 :\ \mathbb{R}^2 \to \mathbb{R}^2$ is defined as

$$h_2 \triangleq \begin{bmatrix} \dot{\xi} \\ \dot{\psi} \end{bmatrix}. \tag{38}$$

Using a similar argument to that made in Theorem 1, leveraging (22), substituting (17), (18), and (38) into the result, and using Property 7, yields

$$\dot{\tilde{V}}_2 \subseteq \psi\left(\chi_2 - \tau_m - B_e K[u_1] - \xi\right) + \xi\left(\psi - \beta\xi\right). \tag{39}$$

After using (19), (39) can be expressed as

$$\dot{\tilde{V}}_2 \subseteq -\beta\xi^2 + \psi\chi_2 - k_6\psi^2 - \psi\tau_m - \Big(k_7 + k_8 \|\phi\| + k_9 \|\phi\|^2\Big)|\psi|. \tag{40}$$

Using Properties 1-6 and the fact that $\dot{V}_2(\zeta) \overset{a.e.}{\in} \dot{\tilde{V}}_2(\zeta)$, (40) can be upper bounded as

$$\dot{V}_2 \overset{a.e.}{\leq} |\psi|\,|\tau_m| - \beta\xi^2 - k_6\psi^2 - |\psi|\left(\lambda_4 + \lambda_5\,\|\phi\| + \lambda_6\,\|\phi\|^2\right), \quad (41)$$

where $\lambda_4,\ \lambda_5,\ \lambda_6 \in \mathbb{R}$ are defined as $\lambda_4 \triangleq k_7 - c_4,\ \lambda_5 \triangleq k_8 - c_5,\ \lambda_6 \triangleq k_9 - c_6$. Provided the gain conditions in (37) are satisfied, $\lambda_4,\ \lambda_5,\ \lambda_6 \geq 0$; thus, (41) can be upper bounded as

$$\dot{V}_2 \overset{a.e.}{\leq} |\psi|\,|\tau_m| - \delta\,\|\zeta\|^2, \quad (42)$$

where $\delta \triangleq \min(k_6,\ \beta)$. Hence, by [17, Definition 6.3] the robot system is output strictly passive with input $|\tau_m|$, output $|\psi|$, and storage function V_2. When the robot acts in isolation (i.e., the human is decoupled from the robot), $\tau_m = 0$, and (42) can be rewritten as

$$\dot{V}_2 \overset{a.e.}{\leq} -\Gamma V_2, \quad (43)$$

where Γ was defined previously. Hence, the storage function qualifies as a radially unbounded positive definite Lyapunov function per the zero-state observability condition [17, Definition 6.5] and results in global exponential stability when $\tau_m = 0$ and $q \in Q_M$. With no human interaction, the admitted trajectories will remain at zero and $\xi \equiv e$, $\psi \equiv r$, and $\zeta \equiv z$. These relations, along with (23) and (43), can be used to obtain the result in (36). From the closed-loop error system in (20), the admittance relation in (15), and Assumption 1, the robot admittance controller in (19) is bounded. □

EXPERIMENTS

Experimental Testbed

Experiments were conducted on a stationary TerraTrike Rover recumbent tricycle with an electric motor coupled to the drive chain. The testbed used an ADVANCED Motion Controls[3] (AMC) power supply, motor driver, and filter card; additional details are available in [2]. Biphasic, symmetric, rectangular pulses were delivered to the rider's muscle groups via bipolar, self-adhesive, PALS® electrodes [4] and a Hasomed Rehastim 1 current-controlled stimulator. Stimulation amplitudes were fixed at 90, 80, and 70 mA for the quadriceps, hamstrings, and gluteals, respectively, with the current determined by the controller in (12). A stop button was available to the rider at all times.

[3]ADVANCED Motion Controls supported the development of this testbed by providing discounts on their branded items.

[4]Surface electrodes for this study were provided compliments of Axelgaard Manufacturing Co., Ltd.

Experimental Methods

The experimental protocol was approved by the Institutional Review Board at the University of Florida. The protocol duration was 180 seconds with the first 30 seconds consisting of a motor-only ramp to the desired cadence of 50 RPM. Two 25 year old males participated in the experiment to demonstrate the efficacy of the controller. Participant 1 was an able-bodied individual; Participant 2 had spina bifida (L5-S1) with an Arnold Chiari Malformation and uses ankle-foot orthoses on both feet along with a wheelchair. Participant 2 actively participates in both physical and occupational therapy and has had previous exposure to FES cycling. Both participants were instructed to remain passive, contribute no volitional torque, and were blind to the desired trajectory; only the quadriceps femoris muscles were used for feasibility purposes.

Results and Discussion

In Participants 1 and 2, the controllers achieved an average cadence of 49.93 ± 2.59 RPM and 49.80 ± 3.86 RPM, respectively, which is equivalent to an average percent error of 0.14% and 0.40%, respectively. The average admitted cadence for Participants 1 and 2 was -0.10 ± 0.40 RPM and -0.20 ± 0.60 RPM, respectively, with cadence tracking results displayed in Figs. 1 and 2. To facilitate gain selection, k_1-k_4 were separated into muscle and motor counterparts; therefore let $k_{i,m} \in \mathbb{R}_{>0}\ \forall i = 1,\ 2,\ \ldots, 4$ refer to the muscle gains in (12) and let $k_{i,e} \in \mathbb{R}_{>0}\ \forall i$ refer to the motor gains in (13). For Participant 1, a feedforward term of 40 μs was added to (12) with $k_{1,m} \triangleq 90$, and for Participant 2, a feedforward term of 20 μs was added with $k_{1,m} \triangleq 40$. The remaining gains were consistent across participants and selected as $k_{2,m} = k_{3,m} \triangleq 0.01$, $k_{4,m} \triangleq 0.005$, $k_5 \triangleq 1$, $k_{1,e} \triangleq 1.8$, $k_{2,e} = k_{3,e} \triangleq 0.01$, $k_{4,e} = 0.005$, $k_6 \triangleq 2$, $k_7 = k_8 \triangleq 0.01$, $k_9 \triangleq 0.005$, $\alpha = \beta \triangleq 1$. The admittance parameters for Participant 1 were selected as $M_d = 0.1 \frac{Nm}{rad \cdot s^2}$ and $B_d = 10 \frac{Nm}{rad \cdot s}$ and for Participant 2 as $M_d = 0.1 \frac{Nm}{rad \cdot s^2}$ and $B_d = 5 \frac{Nm}{rad \cdot s}$. For both participants, the stimulation was saturated at 120 μs for comfort. In the FES regions, the admittance controller tracked a modified admitted trajectory based on the interaction torque measured between the cycle and participant. Because the control objective of the experiment is quantified in terms of cadence, the admittance damping parameter notably affects the performance of the cycle. For example, a low B_d value allows the admitted cadence to deviate from the desired and result in a compliant cycle; a high value of B_d would result in a stiff cycle and hold the admitted cadence close to the desired. This effect is seen in the experimental admitted trajectories between the participants; by halving the damping in Participant 2 compared to Participant 1 (i.e., $5 \frac{Nm}{rad \cdot s}$ from $10 \frac{Nm}{rad \cdot s}$), the admitted cadence doubled (i.e., -0.20 RPM from -0.10 RPM); a more compliant cycle admits more to the rider and will reduce the interaction torque.

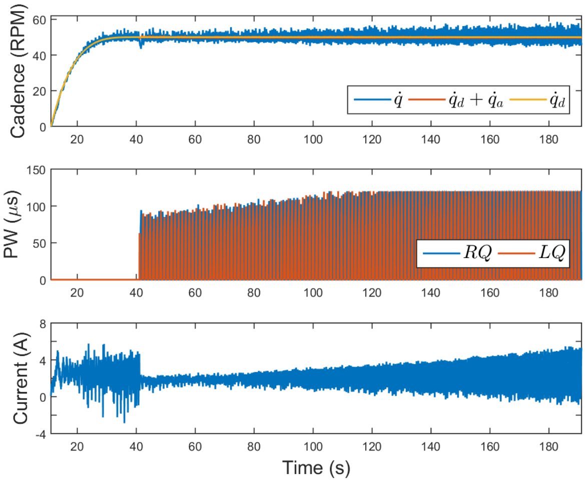

FIGURE 1: PARTICIPANT 1'S CADENCE TRACKING PERFORMANCE. (TOP) THE DESIRED CADENCE COMPARED TO THE ADMITTED AND ACTUAL CADENCE. (MIDDLE) THE PULSEWIDTH (PW) CONTROL INPUTS TO THE PARTICIPANT'S RIGHT AND LEFT QUADRICEPS. (BOTTOM) THE CURRENT CONTROL INPUT TO THE ELECTRIC MOTOR.

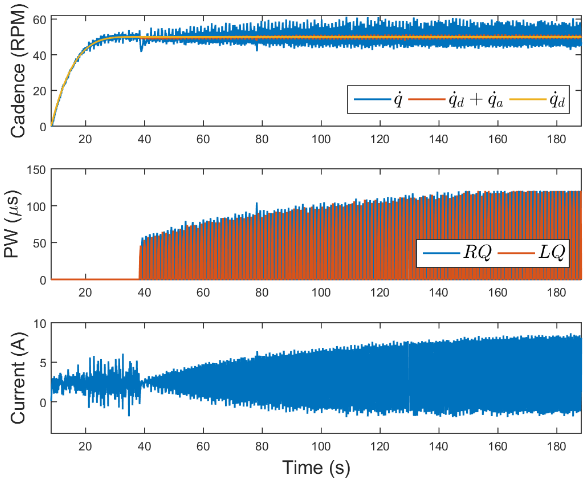

FIGURE 2: PARTICIPANT 2'S CADENCE TRACKING PERFORMANCE. (TOP) THE DESIRED CADENCE COMPARED TO THE ADMITTED AND ACTUAL CADENCE. (MIDDLE) THE PULSEWIDTH (PW) CONTROL INPUTS TO THE PARTICIPANT'S RIGHT AND LEFT QUADRICEPS. (BOTTOM) THE CURRENT CONTROL INPUT TO THE ELECTRIC MOTOR.

CONCLUSION

Robots utilizing admittance control allow for safe, compliant human-robot interaction. Based on the interaction with the human, the robot modifies its own behavior, as dictated by the desired admittance dynamics. This is extremely important in the field of rehabilitation because humans are often in a weakened, unreliable, or unpredictable state. A compliant robot is capable of providing guidance toward control objectives while yielding to human interaction. By modifying the admittance parameters, behaviors such as high frequency tremor can be suppressed while still allowing for slow deliberate movements. In this paper, a rider and an FES cycle were successfully controlled using a combination of three separate controllers across two interacting systems. A Lyapunov-like switched systems stability analysis proved global exponential cadence tracking and passivity of the cycle with respect to the rider. Experiments demonstrated the efficacy of the developed controller and verified the compliance of the cycle. Future works will include developing an adaptive admittance controller to change admittance parameters online to better accommodate for the rider. Additional experiments will be performed on both able-bodied individuals and individuals possessing neurological/movement disorders. The admittance parameters affect the performance of the cycle, however, they are were selected such that favorable cycling performance was achieved; additional investigation will add a desirable interaction torque such that the muscles are performing a useful amount of work for purposes of strength training.

REFERENCES

[1] Bellman, M. J., Cheng, T. H., Downey, R. J., Hass, C. J., and Dixon, W. E., 2016. "Switched control of cadence during stationary cycling induced by functional electrical stimulation". *IEEE Trans. Neural Syst. Rehabil. Eng.,* **24**(12), pp. 1373–1383.

[2] Duenas, V. H., Cousin, C. A., Parikh, A., Freeborn, P., Fox, E. J., and Dixon, W. E., to appear. "Motorized and functional electrical stimulation induced cycling via switched repetitive learning control". *IEEE Trans. Control Syst. Tech.*

[3] Bélanger, M., Stein, R. B., Wheeler, G. D., Gordon, T., and Leduc, B., 2000. "Electrical stimulation: can it increase muscle strength and reverse osteopenia in spinal cord injured individuals?". *Arch. Phys. Med. Rehabil.,* **81**(8), pp. 1090–1098.

[4] Mohr, T., Pødenphant, J., Biering-Sørensen, F., Galbo, H., Thamsborg, G., and Kjær, M., 1997. "Increased bone mineral density after prolonged electrically induced cycle training of paralyzed limbs in spinal cord injured man". *Calcif. Tissue Int.,* **61**(1), pp. 22–25.

[5] Krebs, H. I., and Volpe, B. T., 2015. "Robotics: A rehabilitation modality". *Curr. Phys. Med. Rehab. Rep.,* **3**(4), pp. 243–247.

[6] Cousin, C., Duenas, V. H., Rouse, C., and Dixon, W. E., 2017. "Motorized functional electrical stimulation for torque and cadence tracking: A switched lyapunov approach". In Proc. IEEE Conf. Decis. Control, pp. 5900–5905.

[7] Hunt, K. J., Hosmann, D., Grob, M., and Saengsuwan, J., 2013. "Metabolic efficiency of volitional and electrically stimulated cycling in able-bodied subjects". *Med. Eng. Phys.,* **35**(7), July, pp. 919–925.

[8] Hunt, K. J., Fang, J., Saengsuwan, J., Grob, M., and Laubacher, M., 2012. "On the efficiency of FES cycling: A framework and systematic review". *Technol. Health Care,* **20**(5), pp. 395–422.

[9] Duffell, L. D., Donaldson, N. d. N., and Newham, D. J., 2010. "Power output during functional electrically stimulated cycling in trained spinal cord injured people". *Neuromod. Technol. Neural Interface,* **13**(1), pp. 50–57.

[10] Bo, A. P. L., Fonseca, L., Guimaraes, J., Fachin-Martins, E., Paredes, M. E. G., Brindeiro, G. A., de Sousa, A. C. C., Dorado, M. C., and Ramos, F., 2017. "Cycling with spinal cord injury: A novel system for cycling using electrical stimulation for individuals with paraplegia, and preparation for cybathlon 2016". *Robot Autom. Mag.*

[11] Wiesener, C., and Schauer, T., 2017. "The cybathlon rehabike: Inertial-sensor-driven functional electrical stimulation cycling by team hasomed". *Robot. Autom. Mag.,* **24**(4), pp. 49–57.

[12] Duenas, V. H., Cousin, C., Ghanbari, V., and Dixon, W. E., 2018. "Passivity-based learning control for torque and cadence tracking in functional electrical stimulation (FES) induced cycling". In Proc. Am. Control Conf.

[13] Bellman, M. J., Downey, R. J., Parikh, A., and Dixon, W. E., 2017. "Automatic control of cycling induced by functional electrical stimulation with electric motor assistance". *IEEE Trans. Autom. Science Eng.,* **14**(2), April, pp. 1225–1234.

[14] Hogan, N., 1985. "Impedance control: An approach to manipulation: Part I-theory, part II-implementation, part III-applications". *J. Dyn. Sys., Meas., Control,* **107**(1), Mar., pp. 1–24.

[15] Ranatunga, I., Lewis, F. L., Popa, D. O., and Tousif, S. M., 2017. "Adaptive admittance control for human–robot interaction using model reference design and adaptive inverse filtering". *IEEE Trans. Control Sys. Tech.,* **25**(1), pp. 278–285.

[16] Lee, H., and Hogan, N., 2016. "Essential considerations for design and control of human-interactive robots". In Int. Conf. Robot. Autom., IEEE, pp. 3069–3074.

[17] Khalil, H. K., 2002. *Nonlinear Systems*, 3 ed. Prentice Hall, Upper Saddle River, NJ.

[18] Bellman, M. J., Cheng, T.-H., Downey, R. J., and Dixon, W. E., 2014. "Stationary cycling induced by switched functional electrical stimulation control". In Proc. Am. Control Conf., pp. 4802–4809.

[19] Bellman, M. J., Cheng, T.-H., Downey, R., and Dixon, W. E., 2014. "Cadence control of stationary cycling induced by switched functional electrical stimulation control". In Proc. IEEE Conf. Decis. Control.

[20] Kawai, H., Bellman, M. J., Downey, R. J., and Dixon, W. E., 2014. "Tracking control for FES-cycling based on force direction efficiency with antagonistic bi-articular muscles". In Proc. Am. Control Conf., pp. 5484–5489.

[21] Cousin, C., Duenas, V. H., Rouse, C., and Dixon, W. E., 2018. "Admittance trajectory tracking using a challenge-based rehabilitation robot with functional electrical stimulation". In Proc. Am. Control Conf.

[22] Bellman, M., 2015. "Control of cycling induced by functional electrical stimulation: A switched systems theory approach". PhD thesis, University of Florida.

[23] Tee, K. P., Yan, R., and Li, H., 2010. "Adaptive admittance control of a robot manipulator under task space constraint". In IEEE Int. Conf. Robot. Autom., IEEE, pp. 5181–5186.

[24] Liberzon, D., 2003. *Switching in Systems and Control*. Birkhauser.

[25] Filippov, A. F., 1964. "Differential equations with discontinuous right-hand side". In *Fifteen papers on differential equations*, Vol. 42 of *American Mathematical Society Translations - Series 2*. American Mathematical Society, pp. 199–231.

[26] Paden, B. E., and Sastry, S. S., 1987. "A calculus for computing Filippov's differential inclusion with application to the variable structure control of robot manipulators". *IEEE Trans. Circuits Syst.,* **34**(1), Jan., pp. 73–82.